Dyes and Pigments 90 (2011) 21–27

Contents lists available at ScienceDirect

Dyes and Pigments

journal homepage: www.elsevier.com/locate/dyepig

Clay-assisted dispersion of organic pigments in water

Yi-Fen Lan [a], Jiang-Jen Lin [a,b,*]

[a] Institute of Polymer Science and Engineering, National Taiwan University, No. 1, Sec. 4, Roosevelt Rd., Taipei 10617, Taiwan
[b] Department of Materials Science and Engineering, National Chung Hsing University, No. 250, Kuo Kuang Rd., Taichung 40227, Taiwan

ARTICLE INFO

Article history:
Received 6 October 2010
Received in revised form
11 November 2010
Accepted 12 November 2010
Available online 24 November 2010

Keywords:
Geometry
Pigment
Clay
Colloid
Dispersion
Film

ABSTRACT

We reported a new method for dispersing insoluble organic pigments (OPs) in water by simply pulverizing with the selected clay. The smectite clay of synthetic fluorinated mica (Mica) enabled to homogenize the pigments due to its inherent colloidal properties of surface ionic charges and unique plate-like geometric shape in an average dimension of 300 × 300 × 1 nm^3. Five pigments of different colors were homogeneously dispersed in water and maintained their nanoscale particle sizes in *ca.* 70 nm–2 μm. The zeta potential data revealed a strong surface-charge interaction between the OPs and Mica with a noticeable charge measurement varying from −40 mV to −24 mV. For practical applications, the homogeneous dispersion of pigments was mixed with PVA and spin-coated into polymer films exhibiting the possibility of fabricating color filters. The process has the advantage of avoiding the conventional uses of organic surfactants and solvents.

1. Introduction

Organic pigments (OPs) have a variety of applications such as colorants for coatings [1], inks [2], plastics [3], cosmetics [4] and color filters [5] in electronic devises, mainly because of the thermal stability and excellent optical properties such as good photosensitivity, brilliance, color strength, transparence, and high thermal stability [6]. Compared to the dyes, the OP materials are known for their insolubility in organic solvents and water due to their inherent aggregation through strong noncovalent bonding interactions. In general, the homogeneity of making pigment dispersion requires a fine grinding process along with the use of organic dispersants for viscosity control and the prevention of particle from further agglomeration [7].

Low molecular-weight surfactants are commonly regarded as the dispersants for homogenizing and stabilizing the pigment particles in organic mediums, but the dispersion method is still suffered from the lack of stability for long-term storage or downstream uses. In addition, copolymers of high molecular weight have been employed as dispersants that could resolve some of the problems through the molecular designs with multiple anchoring functionalities for interacting with the pigment surface and simultaneously with the involved solvents [8,9]. For example, the copolymers consisting of random, A–B block and comb-like structures were synthesized and applied successfully for homogenizing the OP dispersion [10–12]. In particular, we have tailored the structures of the acrylic copolymers involving two distinctly different monomers, butyl methacrylate and glycidyl methacrylate by the precise atom-transfer-radical polymerization method [13]. More recently, we have discovered that the new differences in geometric shape could largely affect the nanoparticle dispersions. The inhomogeneity in geometric shapes of any two nanoparticles may also play an important role for excluding each other from aggregation, in other words, the geometric-shape inhomogeneity factor (GIF). The GIF effect was generalized for many different nanomaterials including carbon nanotubes (CNTs) [14], carbon blacks (CBs) [15], carbon nanocapsules (CNCs) [16], silver nanoparticles (AgNPs) [17], iron nanoparticles (FeNPs) [18], and hydrophobic conjugated polymers (CPs) [19,20]. These results had demonstrated the uniqueness of using the synthetic fluorinated mica (Mica) consisting of the fluorinated functionalities, high aspect-ratio, and negative surface charge on surface. Herein, we report that the dispersion of insoluble organic pigments including

Abbreviations: Organic pigments, OPs; Geometric-shape inhomogeneity factor, GIF; Carbon nanotubes, CNTs; Carbon blacks, CBs; Carbon nanocapsules, CNCs; Silver nanoparticles, AgNPs; Iron nanoparticles, FeNPs; Conjugated polymers, CPs; Synthetic fluorinated mica, Mica; Polyvinyl alcohol, PVA; Ultraviolet–visible, UV–vis; Transmission electron microscope, TEM.

* Corresponding author. Institute of Polymer Science and Engineering, National Taiwan University, No. 1, Sec. 4, Roosevelt Rd., Taipei 10617, Taiwan. Tel.: +886 4 2285 7771; fax: +886 4 2285 4332.
E-mail addresses: d95549006@ntu.edu.tw (Y.-F. Lan), jiangjenlin@gmail.com (J.-J. Lin).

0143-7208/$ – see front matter © 2010 Elsevier Ltd. All rights reserved.
doi:10.1016/j.dyepig.2010.11.007

C.I. pigment red 177, green 36, blue 15, yellow 138 and violet 23 in water has been achievable by using plate-like Mica clay. The process involves a simple pulverization of both nanomaterials in powder form and the assistance of ultrasonic agitation to form homogeneous pigment/clay dispersion in aqueous medium. Their dispersion behaviors were further characterized by the means of ultraviolet–visible spectroscope, particle size analyzer, and transmission electron microscope.

2. Experimental section

2.1. Materials

The organic pigments of red, green, blue, yellow and violet (commercial C.I. name: Pigment Red 177, Pigment Green 36, Pigment Blue 15, Pigment Yellow 138, Pigment Violet 23) were obtained from BASF in powder form, and their chemical structures were provided in Fig. 1 [3,6]. The five pigments are insoluble in water and have particle size *ca.* 1–10 μm. The plate-like smectite clay, synthetic fluorinated mica (Mica, trade name as SOMASIF ME-100), was purchased from CO-OP Chemical Co. (Japan). Mica is irregularly aggregated from their primary units comprising of silicate plate units in a stack [21]. The plate-like structure is polygonal and polydispersed in geometric shape, carrying ionic charges and counter ions ($\equiv SiO^{-}Na^{+}$) between the neighboring plates. The Mica has an average plate dimension of $300 \times 300 \times 1$ nm^3 with negative surface-charge density of 2.1 e/nm^2 [22,23]. Due to the presence of ionic charges, the clay is capable of swelling and gelling in water [24]. The polyvinyl alcohol (PVA), obtained from Chang Chun Petrochemical Co., has an average molecular weight of 74,800 and the degree of hydrolysis at 98–99%.

2.2. Preparation of pigment–clay mixture powder

The preparation of the pigment–clay powder is described below. The mixtures of pigment red 177 (1×10^{-6} kg) and Mica (1×10^{-6} kg) were grinded thoroughly in an agate mortar and pestle. During grinding, the inner wall of the mortar was occasionally scraped with the pestle to ensure a thorough mixing. The powder mixture was dispersed into deionized water at the solid concentration of red pigment (1×10^{-6} kg) in water (0.02 kg). The mixtures of Mica/pigment were prepared at different weight ratios (0.5/1, 1/1, 2/1 and 3/1). During the dispersing procedures, ultrasonic vibration was applied for a period of 120 s, operated on BRANSON 5510R-DTH (135 W, 42 kHz).

2.3. Preparation of pigment–PVA composite film

The preparation of the pigment–PVA composite films is described below. The Mica–pigment dispersions (0.003 kg, 0.025 wt percnt; for pigment in water) with different weight fraction (Mica/pigment = 0.5/1, 1/1, 2/1 and 3/1) were dispersed in an aqueous mixture of PVA solution (0.001 kg, 10 wt% PVA in water). The mixture solutions were spun onto 5 × 5 mm glass substrates and dried at 100 °C for 3 h.

2.4. Characterization

The aqueous dispersions of the pigment/clay hybrid were analyzed by ultraviolet–visible spectrophotometer (Perkin–Elmer Lambda 20 UV–vis spectrophotometer) and transmission electron microscope (TEM; JOEL JEM-1230 TEM with Gatan Dual Vision CCD Camera and operated at 100 kV). The TEM samples were prepared by dropping the dispersion of 0.02 wt% pigment/clay onto a carbon-coated copper grid and dried at room temperature. ZetaPlus zetameter (Brookhaven Instrument Corp., NJ) was used for characterizing the ionic property of the pristine clays and pigment/clay mixtures. The pH of the suspension was adjusted to pH 7 by either adding 0.5 M NaOH or HCl. The zeta potential was measured in the solution with an ionic strength of 0.2. The same instrument was used to estimate the average particle size and distribution of the mixture powder in water.

3. Results and discussion

Organic pigments are inherently water-insoluble and usually can only be rendered dispersible by using organic surfactants or copolymers to facilitate downstream processing [8–13]. Recently, we reported a physical method to ease the serious aggregation of these nanomaterials such as CNTs, CBs, CNCs, AgNPs, FeNPs and CPs [14–20]. In these developments, among various clays, the synthetic fluorinated mica (Mica) is found to be mostly suitable for enhancing

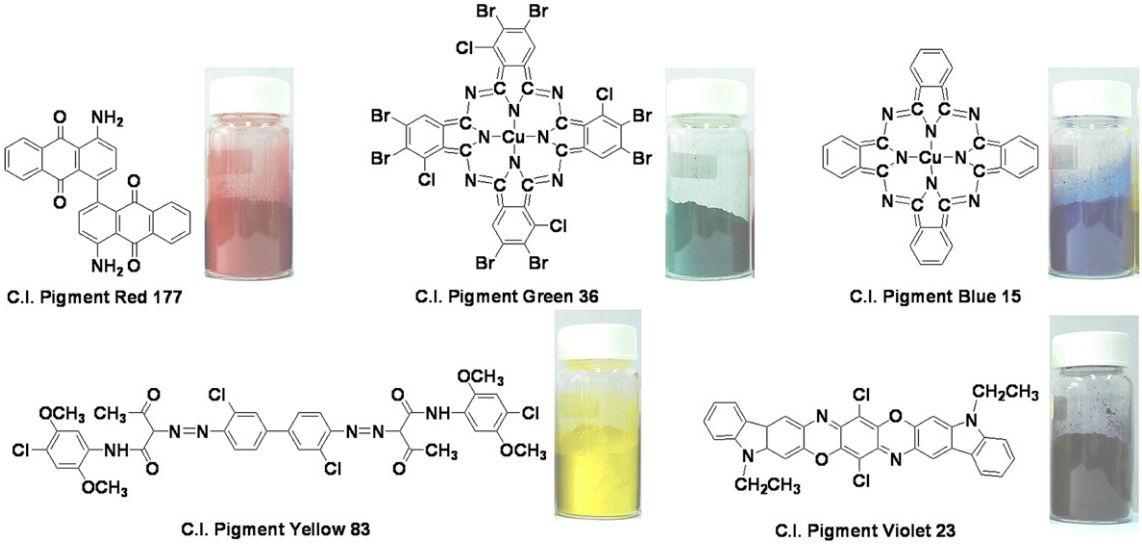

Fig. 1. Chemical structures and color appearance of pigment raw materials. (For interpretation of the references to color in this figure legend, the reader is referred to the web version of this article.)

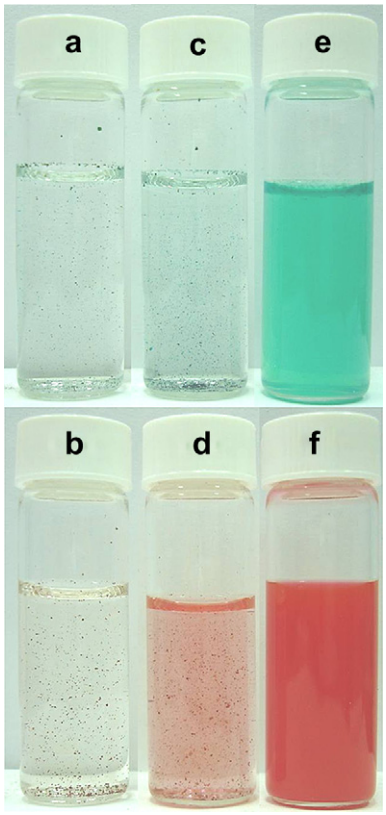

Fig. 2. Visual pictures of dispersing pigments red 177 and green 36 in water (a,b), and with grinding treatment and vigorous agitation before adding water (c,d). The pigment was treated by grinding with Mica at weight ratio of 1/1 and water dispersion (e,f). (For interpretation of the references to color in this figure legend, the reader is referred to the web version of this article.)

the dispersion. When using the clays as the dispersing agents, the mixture of organic pigments and plate-like Mica actually demonstrated a fine dispersion of pigment–Mica in aqueous medium in contrast to the difficulty for mixing the pristine pigments in water. As shown in Fig. 2, the pristine pigment red 177 and green 36 were inherently insoluble in deionized water (Fig. 2a,b). After being vigorously grinded the pristine pigment and the fine pigment powder still lacked of dispersion remained as severe precipitation (Fig. 2c,d). For comparison, the fine dispersion of pigment was achievable by grinded with the added plate-like Mica before the water mixing and the resultant solution remained homogeneous with colorful appearance of red or green (Fig. 2e,f).

In order to understand the effect of Mica clay on pigment particles, the commercial products of blue 15 and red 177 were chosen for the screening. The powder mixtures of pigment–Mica (weight ratio of Mica/pigment = 0.5/1, 1/1, 2/1, and 3/1) were prepared and then dispersed in the water. In Fig. 3, the visual observation of pigment dispersion with different amount of Mica in water can be differentiated by naked eyes. For example, the Mica/blue mixture at 0.5/1 weight ratios only showed slight suspension of the color pigment in water. However, with the increased amount of Mica addition at weight ratios of Mica/blue set at 1/1, 2/1 and 3/1, the blue color deepened due to the homogeneous dispersion (Fig. 3a). The same trend was observed when the red pigment was dispersed into water at the presence of Mica (Fig. 3b).

The ability of Mica affecting the pigment dispersion was characterized by UV–vis absorption method. In Fig. 3c,d, it is shown that the intensity of absorbance for the blue and red pigments increased with the increasing amount of Mica [14]. For the controlled experiment, the solution of the pristine Mica dispersion in water has no of absorbance at wavelength of 400–800 nm [19]. With the presence of Mica, the enhanced dispersion had reached the plateau or nearly maximum at 1/1 ratio for the blue and red pigments. This indicates that the aggregation of pigment has been effectively overcome by the Mica interaction.

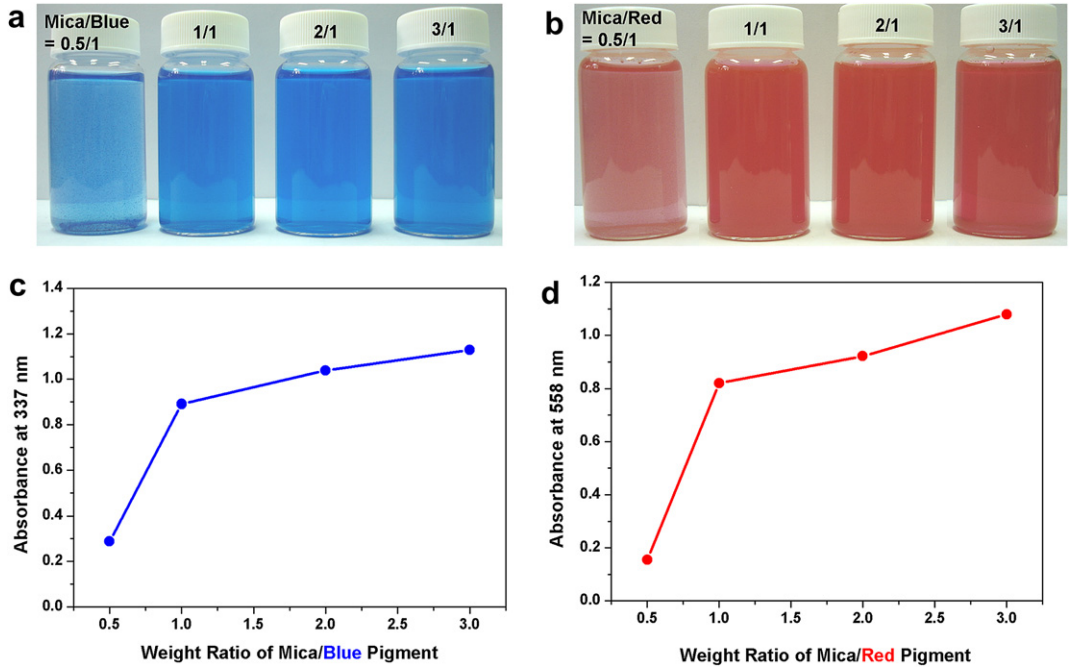

Fig. 3. Visual observation of the dispersions with pigment blue 15 (a) and red 177 (b) at various amounts of Mica presence and their corresponding UV–vis absorbance at wavelength of 337 nm (c) and 558 nm (d). (For interpretation of the references to color in this figure legend, the reader is referred to the web version of this article.)

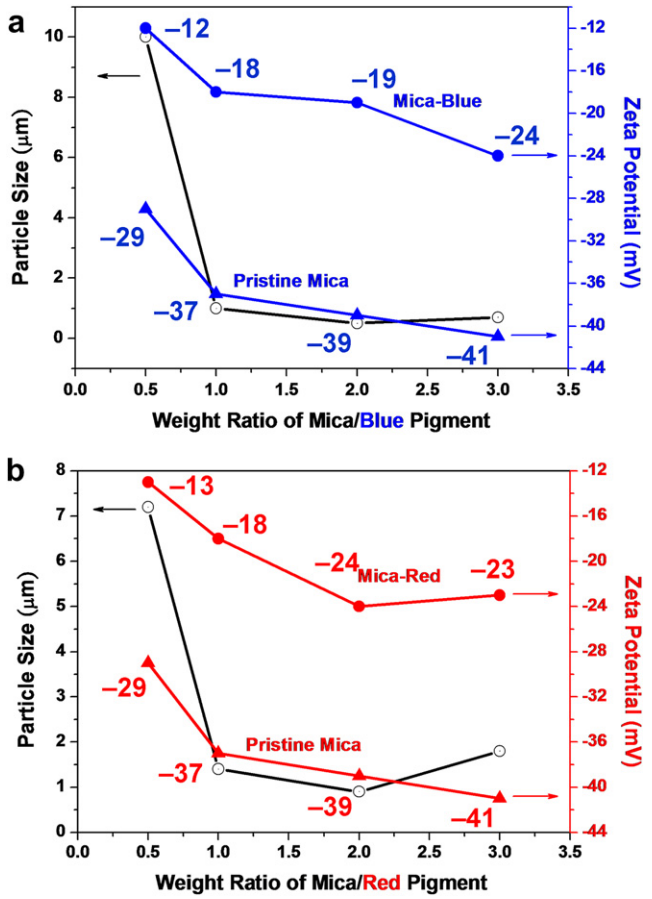

Fig. 4. Particle size and zeta potential analyses of the dispersion of Mica–pigment blue 15 (a) and red 177 (b) in water. (For interpretation of the references to color in this figure legend, the reader is referred to the web version of this article.)

The performance of plate-like Mica for enabling the dispersion of the representative blue and red pigments is examined by Zeta-Plus zetameter and summarized in Fig. 4. After plate-like Mica being added and adequately milled, the pigment was homogeneously dispersed in water. The results of particle size analyzer and zeta potential showed the average aggregated size of pigment has been significantly improved. For example, the particle size and zeta potential of Mica/blue were 7.2 μm and −12 mV for Mica/blue = 0.5/1, 1.4 μm and −18 mV for 1/1, 0.9 μm and −19 mV for 2/1, and 1.8 μm and −24 mV for 3/1 (Fig. 4a). For Mica/red hybrids, the solutions have the similar dispersion trend of 10 μm and −13 mV for 0.5/1, 1.0 μm and −18 mV for 1/1, 0.5 μm and −24 mV for 2/1, and 0.7 μm and −23 mV for 3/1 (Fig. 4b). By comparison, the pristine Mica has the zeta potential of −39 mV. The zeta potential of Mica/blue at weight ratio of 2/1 rendered a significant positive change from −39 mV to −19 mV, indicated the surface-charge interaction between blue pigment and Mica (Fig. 4a). For the red pigment, the zeta potential also revealed a positive change from −39 mV to −24 mV because of the Mica interaction. Both of blue and red pigments exhibited a positive change in zeta potential due to the strong interaction between pigment and Mica plate.

The particle size and its distribution could be characterized (Fig. 5). The result of particle size distribution was highly correlated to the analysis of particle size measurement. For example, the particle size measurement and distribution of Mica/blue were 7.2 μm and 8377 nm/9152 nm at Mica/blue = 0.5/1, 1.4 μm and 735 nm at 1/1, 0.9 μm and 474 nm at 2/1, and 1.8 μm and 1058 nm/3554 nm at 3/1. The same trend of size and distribution was showed in Mica/red solutions, 10 μm and 10,000 nm at Mica/red = 0.5/1, 1.0 μm and 439 nm at 1/1, 0.5 μm and 474 nm at 2/1, and 0.7 μm and 472 nm/2430 nm at 3/1. In the case of Mica/blue or Mica/red = 3/1, the dispersion was observed to have a high particle size (or distribution) than at Mica/blue or Mica/red = 2/1 due to the presence of excess Mica which was *ca.* 300–1000 nm [22].

The pigment dispersion in water by the presence of Mica was noticeable by naked eyes as well as measurable by TEM. As shown in Fig. 6, pigments in red, green, blue, yellow, and violet color were homogeneously dispersed in water (Fig. 6 inserted). The TEM micrograms revealed that the particle sizes of pigments are *ca.*

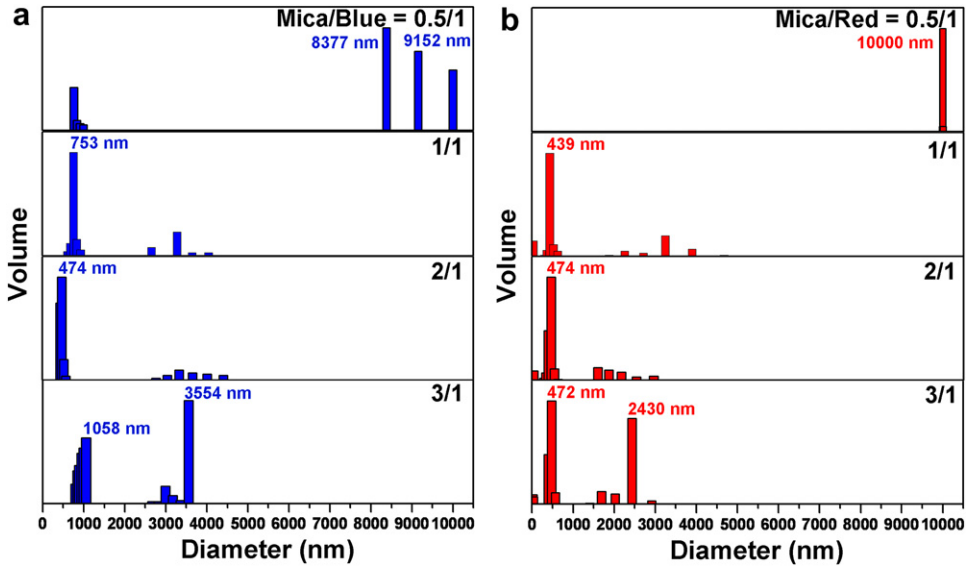

Fig. 5. Size distribution of blue (a) and red (b) pigments in water. (For interpretation of the references to color in this figure legend, the reader is referred to the web version of this article.)

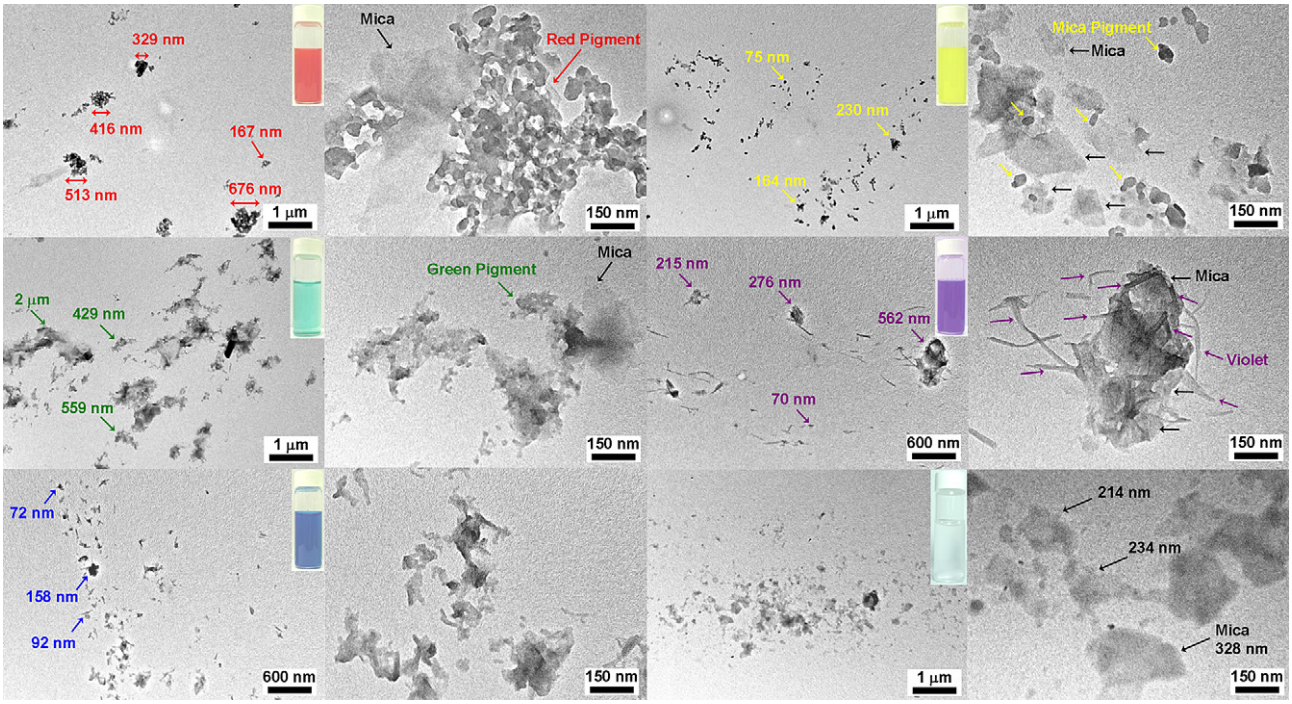

Fig. 6. TEM of dispersions consisting of pigment red 177, green 36, blue 15, yellow 138, violet 23 and pristine Mica in water (weight ratio of Mica/pigment = 1/1). (For interpretation of the references to color in this figure legend, the reader is referred to the web version of this article.)

300–700 nm for red, 0.4–2 μm for green, 70–160 nm for blue, 70–240 nm for yellow and 70–570 nm for violet. Moreover, the geometric shape and size are vividly observed. Irregular shape and particularly rod-like morphology for pigment violet 23, are clearly visualized by using TEM. It is noted that the Mica has an irregular plate shape with average dimension in *ca.* 300 nm [22].

For the possible usage in optoelectronic devices, the pigment–clay dispersion was demonstrated to be dispersible in PVA, as shown in Fig. 7a,b. The fine dispersion can be differentiated by naked eyes for the pigment in PVA solution with a significant improvement in the presence of Mica. For example, the Mica/blue was observed to be aggregates at weight ratio of 0.5/1, by

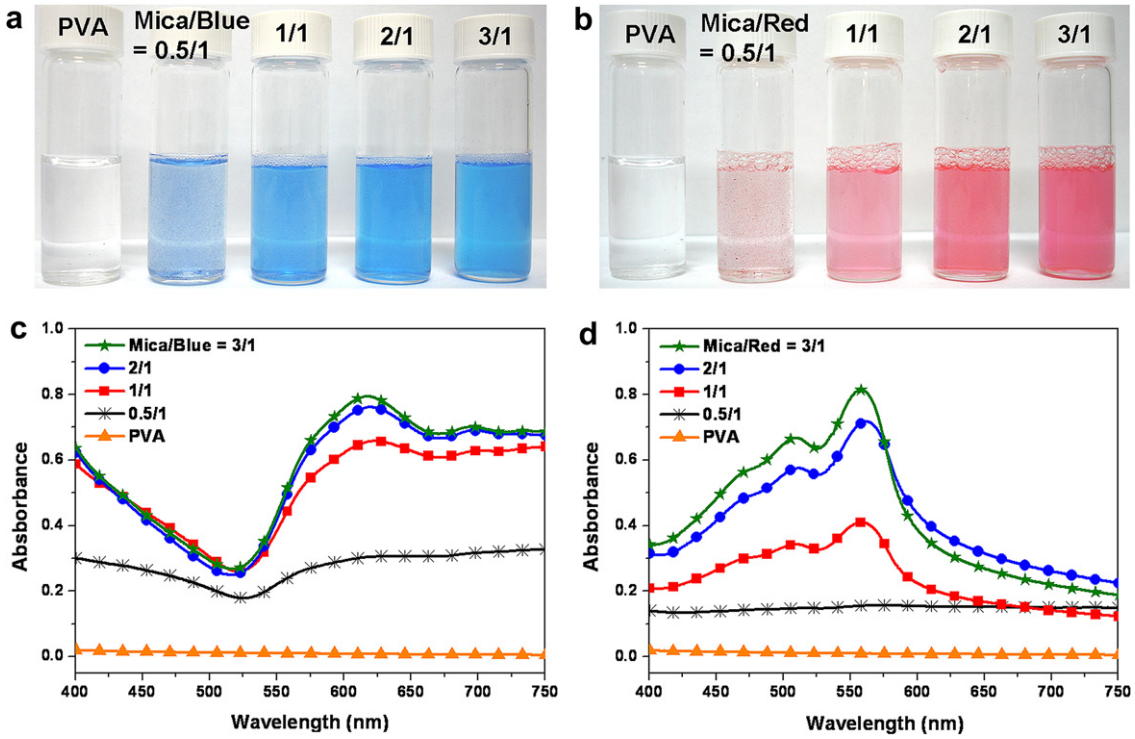

Fig. 7. Visualization of the dispersions for pigment–PVA: blue–PVA (a) and red–PVA (b) at various ratios of Mica/pigment and their UV–vis absorbance of blue (c) and red (d). (For interpretation of the references to color in this figure legend, the reader is referred to the web version of this article.)

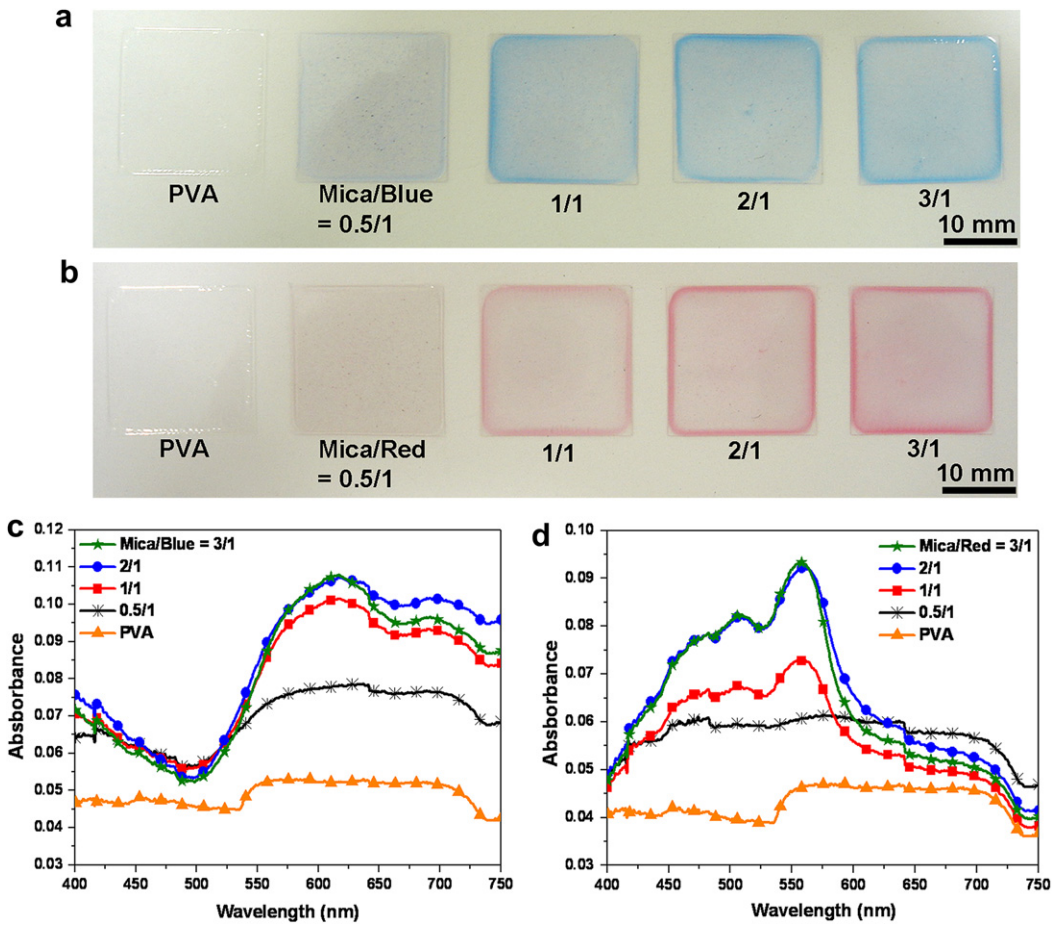

Fig. 8. Visualization of composite films for pigment–PVA: blue–PVA (a) and red–PVA (b) at various ratios of Mica/pigment and their UV–vis absorbance of blue (c) and red (d). (For interpretation of the references to color in this figure legend, the reader is referred to the web version of this article.)

comparison with the homogeneous appearance at 3/1. The same trend was observed for the red pigment. Analyzed by UV–vis, the blue–PVA solution has a broad absorption at 625 nm, while the absorbance intensified with increasing Mica amount, an indication of improvement in dispersion (Fig. 7c). The same phenomenon was shown for the red–PVA dispersion but different absorption peaks (Fig. 7d).

The PVA dispersion was further coated into Mica–pigment–PVA films. While the original PVA film is shown to be transparent and colorless (Fig. 8), the pigment–PVA composite films have a inhomogeneous aggregates with a light blue appearance at Mica/blue weight ratio of 0.5/1 (Fig. 8a,b). At the weight ratio from 1/1 to 3/1, the composite film is homogeneous for the blue pigment distribution and in deep blue appearance. It is similarly observed for the red–PVA films. The solid films were further analyzed by using UV–vis spectrophotometer (Fig. 8c,d) and shown to have similar absorption as in dispersion or in Fig. 7c,d. The increasing amount of Mica demonstrated the homogeneous blue films and an intensive but broad absorption at 625 nm. The absorbance intensity increased with increasing Mica amount, indicating the improvement of dispersion in PVA matrix (Fig. 8c). For the red–PVA films, they demonstrated strong and broad absorption at 550 nm intensified with increasing Mica amount.

4. Conclusion

In conclusion, the use of inorganic Mica demonstrated the improvement of insoluble pigment dispersion in water mainly due to their difference in geometric shape. The dispersion method was generalized for C.I. pigments, red 177, green 36, blue 15, yellow 138 and violet 23, enabled by the Mica clay with geometric plate shape, high aspect-ratio and intensive surface charge. By the simple process of pulverization of pigment and Mica, the mixture became dispersible in water with particle size controllable at *ca.* 70 nm–2.0 μm. The zeta potential measurements had revealed the presence of strong surface-charge attraction between pigment and Mica particles, implying another important factor of charge interaction. With the PVA addition, the dispersion was further coated onto film with different pigment colors and demonstrated the effectiveness of Mica clay. Through the Mica interaction, the difficulty of dispersing pigment in water is overcome, and the feasibility of utilizing pigments without organic solvent is evidenced.

Acknowledgements

We acknowledge financial supports from the Ministry of Economic Affairs and National Science Council (NSC) of Taiwan.

References

[1] Van ST, Velamakanni BV, Adkins RR. About coatings and cathodic protection: electrochemical features of coatings used on pipelines. Journal of Coating Technology 2001;73:61–70.
[2] Baez E, Quazi N, Ivanov I, Bhattacharya SN. Stability study of nanopigment dispersions. Advanced Powder Technology 2009;20:267–72.

[3] Hao ZM, Iqbal A. Some aspects of organic pigments. Chemical Society Reviews 1997;26:203–13.
[4] Qu D, Duncan JW. A study on pigment dispersion in color cosmetics: milling process and scale-up. Journal of Cosmetic Science 2000;51:323–41.
[5] Carotenuto G, Her YS, Matijevic E. Preparation and characterization of nanocomposite thin films for optical devices. Industrial & Engineering Chemistry Research 1996;35:2929–32.
[6] Bieleman J. Additives for coatings. Weinheim: Wiley; 2000.
[7] Spinelli HJ. Polymeric dispersants in ink jet technology. Advanced Materials 1998;10:1215–8.
[8] Kuo KH, Peng YH, Chiu WY, Don TM. A novel dispersant for preparation of high loading and photosensitive carbon black dispersion. Journal of Polymer Science Part A: Polymer Chemistry 2008;46:6185–97.
[9] Creutz S, Jerome R. Effectiveness of poly(vinylpyridine) block copolymers as stabilizers of aqueous titanium dioxide dispersions of a high solid content. Langmuir 1999;15:7145–56.
[10] Burke NAD, Stover HDH, Dawson FP. Magnetic nanocomposites: preparation and characterization of polymer-coated iron nanoparticles. Chemistry of Materials 2002;14:4752–61.
[11] Kang YT, Taton A. Controlling shell thickness in core-shell gold nanoparticles via surface-templated adsorption of block copolymer surfactants. Macromolecules 2005;38:6115–21.
[12] Nuopponen M, Tenhu H. Gold nanoparticles protected with pH and temperature-sensitive diblock copolymers. Langmuir 2007;23:5352–7.
[13] Chen YM, Lin HC, Hsu RS, Hsieh BZ, Su YA, Sheng YJ, et al. Thermoresponsive dual-phase transition and 3D self-assembly of poly(N-isopropylacrylamide) tethered to silicate platelets. Chemistry of Materials 2009;21:4071–9.
[14] Lan YF, Lin JJ. Observation of carbon nanotube and clay micellelike microstructures with dual dispersion property. The Journal of Physical Chemistry A 2009;113:8654–9.
[15] Pai YH, Ke JH, Chou CC, Lin JJ, Zen JM, Shieu FS. Clay as a dispersion agent in anode catalyst layer for PEMFC. Journal of Power Sources 2006;163:398–402.
[16] Hwang GL, Tsai SJ, Lin JJ, Lan YF. Carbon nanocapsule-layered silicate hybrid and preparation method thereof. 2010; U.S. Patent 7625952 B2.
[17] Dong RX, Chou CC, Lin JJ. Synthesis of immobilized silver nanoparticles on ionic silicate clay and observed low-temperature melting. Journal of Materials Chemistry 2009;19:2184–8.
[18] Hsu RS, Chang WH, Lin JJ. Nanohybrids of magnetic iron-oxide particles in hydrophobic organoclays for oil recovery. ACS Applied Materials & Interfaces 2010;2:1349–54.
[19] Lan YF, Lee RH, Lin JJ. Aqueous dispersion of conjugated polymers by colloidal clays and their film photoluminescence. The Journal of Physical Chemistry B 2010;114:1897–902.
[20] Lan YF, Hsieh BZ, Lin HC, Su YA, Chan YN, Lin JJ. Poly(N-isopropylacrylamide)-tethered silicate platelets for colloidal dispersion of conjugated polymers with thermoresponsive and photoluminescence properties. Langmuir 2010;26:10572–7.
[21] Pinnavaia TJ. Intercalated clay catalysts. Science 1983;220:365–71.
[22] Chiu CW, Chu CC, Dai SA, Lin JJ. Self-piling silicate rods and dendrites from high aspect-ratio clay platelets. The Journal of Physical Chemistry C 2008;112:17940–4.
[23] Qi G, Yang Y, Yan H, Guan L, Li Y, Qiu X, et al. Quantifying surface charge density by using an electric force microscope with a referential structure. The Journal of Physical Chemistry C 2009;113:204–7.
[24] Lin JJ, Chen YM. Amphiphilic properties of poly(oxyalkylene)amine-intercalated smectite aluminosilicates. Langmuir 2004;20:4261–4.